Towards the Control of Power Dissipation through the use of Many-Body Coulomb Correlations

G. Albareda, F. Traversa, A. Benali, and X. Oriols
Electronic Engineering Department
Universitat Autònoma de Barcelona. Bellaterra, Barcelona 08193
Email: guillem.albareda@uab.cat

***Abstract*—Power dissipation constitutes a major constriction in modern and future nanoelectronic design [1]. In this context, predictive models elucidating new criterions to control Joule heating would be valuable. In this work we reveal how an accurate formulation of the many-body Coulomb correlations among carriers can lead to new perspectives on the design of power-optimized electron devices. In particular, we show that for a ballistic semi-classical system the rate at which carriers gain (or loose) kinetic energy is a function of carrier-carrier correlations and differs in general from the expected value $\langle I\rangle\cdot\langle\Delta V\rangle$.**

I. Introduction

Most electron transport models assume electron-phonon interaction as the only one mechanism of energy transfer among device's constituent degrees of freedom. Therefore, in ballistic scenarios energy is considered to be a constant of movement for each electron and the amount of kinetic energy gained by the carriers in the active regions to be ultimately transferred as heat to the drain at a rate equal to $\langle I\rangle\cdot\langle\Delta V\rangle$ [2], [3].

However, while shrinking device dimensions reduces the number of carrier-phonon collisions along the device active region, the closer proximity of the high-density source, drain, and gate regions unavoidably increases the strength of carrier-carrier interaction, so that reaching ballistic transport may remain unattainable [4]. In this context, energy is no longer a constant of motion for carriers even if their mean-free path is larger than the device active region. The rate of gain of kinetic energy in the (open) active region is no longer $\langle I\rangle\cdot\langle\Delta V\rangle$ but a direct function of carrier-carrier correlations. It is in this regard that, since inter-particle collisions simply redistribute the momentum among carriers, electron correlations could in principle be designed to manipulate the way kinetic energy is distributed along the different regions of electronic devices, and ultimately, use this information to spatially control the power dissipation.

II. Electric Power in Correlated Open Systems

With the aim of identifying the effects that carrier-carrier correlations introduce on the mean value of the electric power, here we simply switch-off electron-phonon interactions, i.e. we condider a ballistic scenario. In this context, the electric power does no longer refer to the rate at which carrier's kinetic energy is transferred to the underlying atomic structure, but defined as the time derivative of the work done by a (self-consistent) electric field over the N carriers composing the electronic device. This is, by definition, the rate at which carriers gain or loose kinetic energy. In what follows we show that when carrier-carrier correlations are taken into consideration, the standard picture in which carriers loose their kinetic energy in the drain at a reate equal to $\langle I\rangle\cdot\langle\Delta V\rangle$ (in ballistic systems) is no longer accurate.

A semi-classical description of the time-evolution of a classical trajectory $\vec{r_k}[t]$ in the real space leads to the standard Hamilton equations of motion

$$\frac{d\vec{p}_k[t]}{dt}=\left[-\vec{\nabla}_{\vec{r}_k}H\left(\{\vec{r}\},\{\vec{p}[t]\}\right)\right]_{\{\vec{r}\}=\{\vec{r}[t]\}}, \tag{1a}$$

$$\frac{d\vec{r}_k[t]}{dt}=\left[-\vec{\nabla}_{\vec{p}_k}H\left(\{\vec{r}[t]\},\{\vec{p}\}\right)\right]_{\{\vec{p}\}=\{\vec{p}[t]\}}, \tag{1b}$$

where electronic conjugate coordinates are collectively denoted in the configuration space by $\{\vec{r}\}=\{\vec{r}_1,...,\vec{r}_N\}$ and $\{\vec{p}\}=\{\vec{p}_1,...,\vec{p}_N\}$. The many-body Hamiltonian in (1) can be simply written as

$$H\left(\{\vec{r}\},\{\vec{p}\}\right)=\sum_{k=1}^{N}\left\{K\left(\vec{p}_k\right)+\frac{q_k}{2}W_k\left(\{\vec{r}\}\right)\right\}, \tag{2}$$

where

$$K\left(\vec{p}_k\right)=\frac{\left(\vec{p}_k\right)^2}{2m_k}, \tag{3a}$$

$$W_k\left(\{\vec{r}\}\right)=\sum_{\substack{j=1\\ j\neq k}}^{N}\frac{q_j}{4\pi\varepsilon\left|\vec{r}_k-\vec{r}_j\right|}, \tag{3b}$$

and q_k, m_k and ε are respectively the charges and effective masses of the carriers and the dielectric permittivity.

From equation (1a), the time-derivative of the kinetic energy of the carriers (3a) can be written as

$$\begin{aligned}P_k(t) &= \frac{dK\left(\vec{p}_k[t]\right)}{dt}\\ &= -q_k\vec{v}_k[t]\cdot\left[\vec{\nabla}_{\vec{r}_k}W_k\left(\{\vec{r}\}\right)\right]_{\{\vec{r}\}=\{\vec{r}[t]\}}\\ &= -q_k\vec{v}_k[t]\cdot\vec{E}_k\left(\{\vec{r}[t]\}\right),\end{aligned} \tag{4}$$

where $\vec{F}_k=-q_k\cdot\vec{E}_k\left(\{\vec{r}[t]\}\right)$ is the electrostatic force acting over electron k.

Under an hydrodynamic approach, the next equality holds

$$q_k\vec{v}_k\left[t\right]\cdot\left[\vec{\nabla}_{\vec{r}_k}W_k\left(\{\vec{r}\}\right)\right]_{\{\vec{r}\}=\{\vec{r}[t]\}}=\frac{dW_k\left(\{\vec{r}\left[t\right]\}\right)}{dt}-$$
$$-q_k\sum_{\substack{j=1\\j\neq k}}^{N}\vec{v}_j\left[t\right]\cdot\left[\vec{\nabla}_{\vec{r}_j}W_k\left(\{\vec{r}\}\right)\right]_{\{\vec{r}\}=\{\vec{r}[t]\}},\quad(5)$$

and introducing it into (4), we can reexpress the rate at which kinetic energy is gained or loosed by each electron as

$$P_k(t)=\frac{dK\left(\vec{p}_k\left[t\right]\right)}{dt}=-\frac{dW_k\left(\{\vec{r}\left[t\right]\}\right)}{dt}+$$
$$+q_k\sum_{\substack{j=1\\j\neq k}}^{N}\vec{v}_j\left[\vec{\nabla}_{\vec{r}_j}W_k\left(\{\vec{r}\}\right)\right]_{\{\vec{r}\}=\{\vec{r}[t]\}}.\quad(6)$$

Looking now at the kinetic energy associated to a volume Ω delimited by the surfaces S_i and S_f both perpendicular to the spatial x axis respectively at x_i and x_f, using (6) we can define the electric power in Ω associated to the $k-th$ electron as

$$P_k(t)|_\Omega=\left.\frac{dK\left(\vec{p}_k\left[t\right]\right)}{dt}\right|_\Omega=$$
$$=-\frac{dW_k\left(\{\vec{r}\left[t\right]\}\right)}{dt}\cdot\theta_{\vec{r}_k[t],x_i}\cdot\theta_{x_f,\vec{r}_k[t]}+$$
$$+q_k\sum_{\substack{j=1\\j\neq k}}^{N}\vec{v}_j\left[\vec{\nabla}_{\vec{r}_j}W_k\left(\{\vec{r}\}\right)\right]_{\{\vec{r}\}=\{\vec{r}[t]\}}\cdot\theta_{\vec{r}_k[t],x_i}\cdot\theta_{x_f,\vec{r}_k[t]},\quad(7)$$

where the function

$$\theta_{\vec{r}_k[t]-x_i}\cdot\theta_{x_f-\vec{r}_k[t]}=\theta\left(\vec{r}_k\left[t\right]-x_i\right)\cdot\theta\left(x_f-\vec{r}_k\left[t\right]\right)$$
$$=\begin{cases}0 & \vec{r}_k\left[t\right]\not\subset\Omega\\ 1 & \vec{r}_k\left[t\right]\subseteq\Omega\end{cases},\quad(8)$$

is zero valued everywhere except in the volume Ω.

Finally, the time average of the kinetic energy gained by the carriers in the volume Ω can be written as

$$\left\langle P(t)\right\rangle_\Omega=\left\langle\sum_{k=1}^{N}\frac{dK\left(\vec{p}_k\left[t\right]\right)}{dt}\right\rangle_\Omega=$$
$$=\lim_{T\to\infty}\frac{1}{T}\Big(\sum_{k=1}^{N}q_k\Delta W_k+$$
$$+\sum_{k=1}^{N}\sum_{\substack{j=1\\j\neq k}}^{N}\int_{t_k^i}^{t_k^f}dt'q_k\vec{v}_j\left[t'\right]\left[\vec{\nabla}_{\vec{r}_j}W_k\left(\{\vec{r}\}\right)\right]_{\{\vec{r}\}=\{\vec{r}[t']\}}\Big),\quad(9)$$

where we have used that the first term on the r.h.s of (8) is a total time-derivative, and thus

$$\Delta W_k=W_k(\{\vec{r}[t_k^f]\})-W_k(\{\vec{r}[t_k^i]\}),\quad(10)$$

with t_k^i, t_k^f respectively the times at which the electron k enters and leaves the volume Ω. In (9) it is implicitly assumed that each electron enters the volume Ω just once. Although this constraint can be easily relaxed, we assumed it just to keep notation as clear as possible.

Equation (9) constitutes the main result of this work and its physical meaning can be interpreted as follows. The rate at which electrons gain kinetic energy in a particular region of space (here the volume Ω) depends on two terms. The first term on the right hand of (9) constitutes essentially a single-particle contribution, while the second one is the main responsible of introducing the effect of electron-electron correlations into the mean value of the electric power. In order to better understand the nature of the above two terms, let us consider two different limits of equation (9).

First of all, let us consider the non-interacting limit of (10), e.g. for very large applied bias. Under this limit, the electrostatic potential $W_k\left(\{\vec{r}\}\right)$ appearing in (9) is no longer a function of the whole coordinate ensemble but just of $\vec{r}_k$, i.e. $W_k\left(\{\vec{r}\}\right)=V\left(\vec{r}_k\right)$. As a consequence, only the first term on the right hand side of (9) is non-zero valued, and we recover the standard expression for the electric power in the limit of single-particle (SP) dynamics, i.e.

$$\left\langle P(t)\right\rangle_\Omega^{SP}=\left\langle\sum_{k=1}^{N}\frac{dK\left(\vec{p}_k\left[t\right]\right)}{dt}\right\rangle_\Omega^{SP}$$
$$=\left\langle I\right\rangle\cdot\left\langle\Delta V\right\rangle_\Omega.\quad(11)$$

Secondly, for those volumes, Ω, large enough to include the highly doped reservoirs of the electronic device, the open region behaves as a closed system and carriers inside and outside it are no longer correlated. Under this limit, it works out that ΔW_k is for each carrier equal to the applied bias, and then we recover again the standard value of the electric power, which is now identical to

$$\left\langle P(t)\right\rangle_\Omega^{Large}=\left\langle\sum_{k=1}^{N}\frac{dK\left(\vec{p}_k\left[t\right]\right)}{dt}\right\rangle_\Omega^{Large}$$
$$=\left\langle I\right\rangle\cdot\left\langle\Delta V\right\rangle_{Bias}.\quad(12)$$

The above two limits shed light on the nature of the two terms conforming the r.h.s of (9) and suggest an interesting question: can a proper design of device's electrostatics be used to redistribute power dissipation along the active region of an electron device?. Cutting up the whole active region of the device into a certain number of volumes Δx, it turns out that if we are able to control the second term in (9), it will be then possible to manipulate the kinetic energy that carriers gain in the different regions Δx of the active region.

In order to better understand the meaning of this proposal, in what follows we intend to simulate a N^+NN^+ nanostructure and put numbers to the difference between equations (9) and (11), and thus get an intuitive picture of the role carrier-carrier Coulomb correlations.

III. Computation of the many-body Coulomb correlations

In order to evaluate expression (9), however, we need to expressly introduce electron-electron Coulomb correlations into our simulations. Since we cannot deal with the whole number of degrees of freedom constituting a whole closed

electronic system, we need, in addition, a many-body approach specific for open systems. We will use a recently presented approach to describe carrier dynamics with the exact electron-electron Coulomb correlations in open systems [5]. Under this approach, the exact many-body Hamiltonian, for classical systems, describing the dynamics of the $N(t)$ carriers enclosed in the active region of an electron device can be defined as:

$$H^{open}\left(\{\vec{r}\}^t,\{\vec{p}\}^t,t\right)= \sum_{k=1}^{N(t)}\left\{K\left(\vec{p}_k\right)+q_k\bar{W}_k\left(\vec{r}_k,t\right)\right\}, \quad (13)$$

where $\{\vec{r}\}^t=\left\{\vec{r}_1,...,\vec{r}_{N(t)}\right\}^t$ and $\{\vec{p}\}^t=\left\{\vec{p}_1,...,\vec{p}_{N(t)}\right\}^t$ are now the ensemble coordinates in the configuration space of the carriers in the active region. The electrostatic potential $\bar{W}_k\left(\vec{r}_k,t\right)$ in (13) is the solution of one particular 3D-Poisson equation,

$$\nabla_{\vec{r}_k}\left[\varepsilon\cdot\nabla_{\vec{r}_k}\bar{W}_k\left(\vec{r}_k,t\right)\right]=-\bar{\rho}_k\left(\vec{r}_k,t\right), \quad (14)$$

where the single-particle charge density can be defined as

$$\bar{\rho}_k\left(\vec{r}_k,t\right)=\sum_{\substack{j=1\\ j\neq k}}^{N(t)} q_j\cdot\delta\left(\vec{r}_k-\vec{r}_j\left[t\right]\right). \quad (15)$$

The solution of the Hamiltonian in (13) together with equations (14) and (15), coupled to an appropriate set of boundary conditions (see Ref. [6]), provides a set of Newton-type equations [5],

$$\frac{d\vec{p}_k\left[t\right]}{dt}=-q_k\vec{\nabla}_{\vec{r}_k}\,\bar{W}_k\left(\vec{r}_k,t\right)\big|_{\vec{r}_k[t]}. \quad (16)$$

Expressions (14) to (16) lead to a set of $N(t)$ Newton equations coupled through $N(t)$ Poisson equations, meaning that each carrier "sees" its own electrostatic potential. This equations provide an exact treatment of the many-body Coulomb correlations in the simulated region. Although the r.h.s of (14) does only depend on the $N(t)$ carriers enclosed in the active region at time t, the dependency of the electrostatic potential $\bar{W}_k\left(\vec{r}_k,t\right)$ on the rest of the $N-N(t)$ carriers can be taken into account by imposing overall charge neutrality over the whole system composed by the active region and the reservoirs [6]. Then, the local continuity equation for the electronic charge leads to a rigorous definition of the (time-dependent) boundary conditions for the Poisson equation in (14). Coupling then these boundary conditions to an appropriate electron injection model is sufficient to introduce quite rigorously the Coulomb correlations among carriers inside and outside the active region of the electron device (more details on the definition of the time-dependent boundary conditions and the injection model can be find in Ref. [6]).

IV. Comparison of the Exact Electric Power with its Single-Particle Limit $\langle I\rangle\cdot\langle\Delta V\rangle$

Finally, provided equations (16) to (15), we are ready to evaluate expression (9). By comparing it with its non-interacting limit (11), we will be able to evaluate the contribution of the many-body Coulomb correlations into the rate

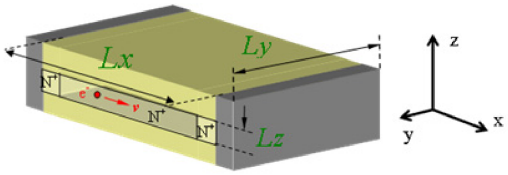

Fig. 1. Schematic picture of the simulated Silicon N^+NN^+ resistor. $N^+=6.25E18, L_x=10nm, L_y=30nm, L_z=30nm$. N referes intrinsic Silicon.

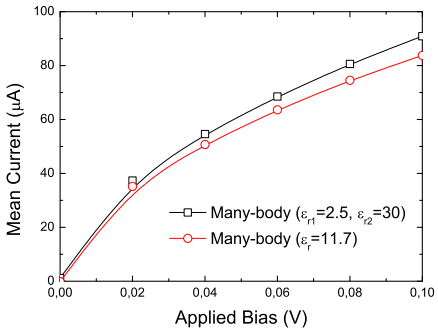

Fig. 2. I vs V characteristics for the nanostructure of Fig. 1 with two different dielectric permittivity spatial distributions. In circles, we consider an intrinsic active region with an homogeneous relative permittivity all long, $\varepsilon_r=11.7$. In squares, we split the active region into two well differentiate regions, both intrinsic, but now with two different relative permittivities, $\varepsilon_r=2.5$ in the left half part of the active region, and $\varepsilon_r=30.0$ in the right half side.

at which electrons gain or loose kinetic energy. As a simple example, we consider here a N^+NN^+ structure with $L_x=10nm, L_y=30nm, L_z=30nm$ and $N^+=6.25E18cm^{-3}$ (see Fig. 1). In order to enlighten the role of the carrier-carrier Coulomb correlations taking place in this nanostructure, we consider two different electrostatic scenarios. On one hand, we consider an intrinsic active region with an homogeneous relative permittivity all long, $\varepsilon_r=11.7$. On the other hand, we split the active region into two well differentiate regions, both intrinsic, but now with two different relative permittivities, $\varepsilon_r=2.5$ in the left half part of the active region, and $\varepsilon_r=30.0$ in the right half side.

In figure 2 we present the characteristic $I(V)$ curves for the two active regions described above. Let us notice that a change on the dielectric permittivity along the active region will not introduce any difference on the mean value of the electrical currents in the saturation region (at very large bias). However, due to intrinsic differences associated to different electrostatic permittivities, the average currents are no longer equal at intermediate bias.

In figures 3 and 4 we represent the spatial distribution of the difference between equation (9) and its non-interacting limit (11) for the two simulated structures. We have split up the active region into 20 infinit volumes Ω with $\Delta x=0.5nm$. Two well differentiate spatial regions can be observed in figure 3, one where (9)-(11)>0, and the other where (9)-(11)<0.

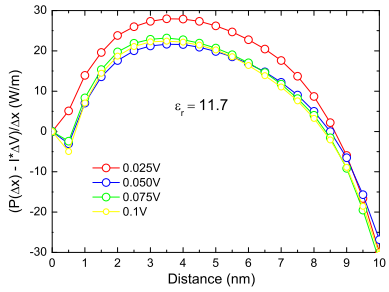

Fig. 3. Spatial distribution of the difference between equation (9) and its non-interacting limit (11) for an homogenious dielectric permittivity. The active region has been split up into 20 infinit contiguous volumes Ω. Carrier "bunching" causes a positive difference between the exact value of the electric power spatial density and its non-interacting limit $\langle I \rangle \cdot \langle \Delta V \rangle$ value. The contrary happens in presence of "antibunching" of carriers.

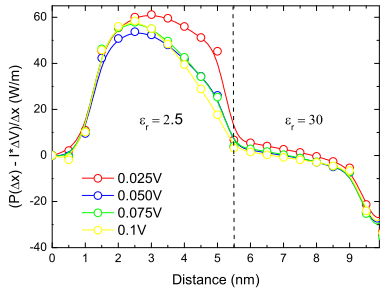

Fig. 4. Spatial distribution of the difference between equation (9) and its non-interacting limit (11) for bipartite dielectric permittivity. The manipulation of the active region electrostatic parameters can be designed to increase bunching and antibunching dynamics. The discrepancy between the kinetic energy gain rate and $\langle I \rangle \cdot \langle \Delta V \rangle$ can be then stressed.

These two regions are placed, one close to the source reservoir and the other close to the drain, indicating that carrier-carrier correlations induce an increase of the rate of kinetic energy gain close to the source and viceversa for those electrons approaching the drain. Intrinsic electrostatic variations induced by a change on the dielectric permittivity clearly affect this many-body behavior. In figure 4, it can be observed how the above deviation from the non-interacting picture (11) can be stressed if we know how to modify intrinsic electrostatics. These results might be better understood by looking at the mean potential energy distribution along the active region. In figure 5 we can see how a spatial variation on the relative permittivity noticeably modifies the conduction band surface. In this regard, it is quite notable that there exists a close correlation between the shapes on figure 5 and those in figures 3 and 4. In this regard, it can be inferred a close relation between the "bunching" and "antibunching" of carriers and the positive and negative signs of the difference (9)-(11).

V. Conclusion

The closer proximity of the high-density source, drain, and gate regions unavoidably increases the strength of carrier-

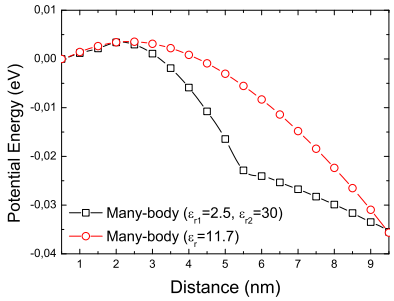

Fig. 5. The manipulation of the active region dielectric permittivity induces a change on the average conduction band distribution that modifies the way carriers interact with each other.

carrier interaction, so that reaching ballistic transport may remain unattainable. In this context, energy is no longer a constant of motion for carriers even if their mean-free path is larger than the device active region. The rate of gain of kinetic energy in the (open) active region is no longer $\langle I \rangle \cdot \langle \Delta V \rangle$ but a direct function of carrier-carrier correlations. In this work we have shown how a proper modification of certain underlying material electrostatic properties such as the dielectric permittivity can help us in controling the way carriers gain or loose kinetic energy, and thus, the way this energy is finally going to heat up the underlying atomic structure. Bunching and antibunching carrier dynamics seem to play a crucial role on the determination of the difference between the many-body electric power and its single-particle limit. Further research must be still devoted to understand the role that carrier-carrier correlations play on the way kinetic energy is gained and finally dissipated in electronic devices. This work opens a new route to study and even to maniulate these variables through a proper design of the underlying structure electrostatic properties.

Acknowledgment

This work has been partially supported by the Ministerio de Ciencia e Innovación under Project No. TEC2009-06986 and by the DURSI of the Generalitat de Catalunya under Contract No. 2009SGR783. G. Albareda also wants to thank both Beatriu de Pinós and Marie Curie programs ($2010BP_A00069$).

References

[1] D.J. Frank *Power-constrained CMOS scaling limits*, IBM J. Res. & Dev. **46**, 235 (2002).
[2] E. Pop *Energy dissipation and transport in nanoscale devices*, Nano Research **3**, 147 (2010).
[3] B. Myung-Ho et al., *Imaging, Simulation, and Electrostatic Control of Power Dissipation in Graphene Devices*, Nano Letters **10**, 4787 (2010).
[4] M.V. Fischetti et al., *Scaling MOSFETs to 10nm: Coulomb effects, source starvation, and virtual source model*, J. Comput. Electron **8**, 60 (2009).
[5] G. Albareda et al., *Many-particle Hamiltonian for open systems with full Coulomb interaction: Application to classical and quantum time-dependent simulations of nanoscale electron devices*, Phys. Rev. B **79**, 075315 (2009).
[6] G. Albareda et al., *Time-dependent boundary conditions with lead-sample Coulomb correlations: Application to classical and quantum nanoscale electron device simulators*, Phys. Rev. B **82**, 085301 (2010).